USED FUEL DISPOSITION CAMPAIGN

Effect of Iodide on Radiolytic Hydrogen Peroxide Generation

Fuel Cycle Research & Development

Prepared for
U.S. Department of Energy
Used Fuel Disposition Campaign

Edgar Buck
Rick Wittman

July 28, 2017

M4SF-17PN010501041

PNNL-26639

Submitted by:

Signature on file

_____

Edgar C. Buck
PNNL

EXECUTIVE SUMMARY

This report fulfills the milestone (M4SF-17PN010501041 Report on Radiolysis Modeling for the Defense Repository) to discuss continued integration of the PNNL Radiolysis Model and the ANL Mixed Potential Model. This work concerns the development of an integrated Radiolysis Model (RM) for evaluating defense waste materials (oxide and metal) degradation and radionuclide mobilization. Within an anoxic repository environment, primary oxidizing species (e.g., hydrogen peroxide (H_2O_2), OH• radicals, as well as chlorate and other oxidizing species depending on the disposal environment) will be generated at the surface of the nuclear waste forms as a function of their specific activity.

RM development has included expansion of chemical environments considered to encompass species for various disposal environments. PNNL has been coordinating this effort with ANL on the integration of the radiolysis work with the fuel degradation model.

RM development at PNNL has expanded to include chemical environments such as bromide, chloride, and carbonate. The model was originally developed for spent fuel degradation but can also encompass other alterative waste forms that will generate long-term (particularly alpha-dominated) radiation fields during disposal. In this report, we discuss potential radiolytic effects on metallic and ceramic waste forms over a range of repository environments. Objectives in this work, include:

- Continued development of a chemical-radiolysis model for predicting the radiolytic speciation at various conditions.
- Implementation of an enhanced radiolysis model coupled to the waste form degradation for in-package chemical conditions focusing on the role of H_2 and other interactions in the defense repository environments.
- Development of potential experimental *in-situ* testing tools to evaluate radiolytic processes and validating modeling efforts.
- Leverage the efforts of other working in the radiolysis area.

In this study, we demonstrate and approximate possible effects of iodide on H_2O_2 generation. As has been shown these are conditions for which H_2O_2 generation is reduced. We find that the presence of the iodide ion reduces the steady-state H_2O_2 concentration, but not to the same degree as bromide at micro-molar concentrations.

We also report on *in-situ* investigations of UO_2 corrosion using liquid cell electron microscopy where the electron beam is utilized as the radiation source generating oxidizing species.

Additionally, suggestions are offered on what further data or measurements would be required for model verification and applicability. The listings of the reactions considered in this report are given in Appendix A and the Fortran modeling code is provided in Appendix B.

ACKNOWLEDGMENTS

We thank Jim Jerden for continued discussions on the operation of the ANL Mixed Potential Model. We thank Carlos Jové-Colón and David Sassani for their continued support of this research and helpful discussions on the effects of radiolysis chemistry and its applicability to model predictions.

CONTENTS

EXECUTIVE SUMMARY v

ACKNOWLEDGMENTS vii

CONTENTS ix

ACRONYMS xii

1. INTRODUCTION 13

2. RADIOLYSIS MODEL WITH IODINE REACTIONS 15
   - 2.1 Effect of Iodide on H_2O_2 in Radiation Zone 15
   - 2.2 Experimental Validation of Radiolysis 17
   - 2.3 Future work 20

3. REFERENCES 21

APPENDIX A: Reaction Listing for Full RM 13

APPENDIX B: FORTRAN Listing for Empirical RM 17

FIGURES

Figure 2-1. Effect of an initial micro-molar and greater concentration of Iodide (solid) and Bromide ions on H_2O_2 generation at 160 rad/s alpha dose rate. 16

Figure 2-2. Effect of an initial micro-molar and greater concentration of Iodide (solid) and Bromide ions on H_2O_2 generation at 25 rad/s alpha dose rate. 17

Figure 2-3 Tracking the dissolution of UO_2 in nitric acid showing how microscopy measurements can determine rates of reaction 18

Figure 2-4 Plot showing change in particle surface area with time 18

Figure 2-5 Electron microscopy images showing the formation of an alteration phase following the irradiation of a solution containing UO_2 particles. 19

ACRONYMS

ANL	Argonne National Laboratory
DIW	de-ionized water
DOE	U.S. Department of Energy
DOE-NE	U.S. Department of Energy Office of Nuclear Energy
MPM	Mixed Potential Model
ODE	ordinary differential equation
PNNL	Pacific Northwest National Laboratory
RM	Radiolysis Model
SNF	spent nuclear fuel
UFDC	Used Fuel Disposition Campaign
UNF	used nuclear fuel

USED FUEL DISPOSITION CAMPAIGN
Effect of Iodide on Radiolytic Hydrogen Peroxide Generation

1. INTRODUCTION

The U.S. Department of Energy Office of Nuclear Energy (DOE-NE), Office of Fuel Cycle Technology has established the Used Fuel Disposition Campaign (UFDC) to conduct the research and development activities related to storage, transportation, and disposal of used nuclear fuel (UNF) and high-level radioactive waste. Within the UFDC, the components for a general system model of the degradation and subsequent transport of UNF is being developed to analyze the performance of disposal options [Sassani et al., 2012]. Two model components of the near-field part of the problem are the ANL Mixed Potential Model and the PNNL Radiolysis Model.

This report is in response to the desire to integrate the two models as outlined in [Buck et al., 2013] "Coupling the Mixed Potential and Radiolysis Models for Used Fuel Degradation," FCRD-UFD-2013-000290, M3FT-PN0806058].

This report gives a comparison on the effect of iodide and bromide chemistry on H_2O_2 generation under radiolytic condition at the surface of used nuclear fuel under repository conditions. Additionally, suggestions are offered on what further data or measurements would be required for model verification and applicability. The listings of the reactions considered in this report are given in Appendix A.

One of the most important reactions for iodine is the direct reaction with H_2O [Buxton and Mulazzani, 2007]:

$$I_2 + H_2O \rightarrow HOI + I^- + H^+ \quad \text{Eq.1}$$
$$3HOI \rightarrow IO_3^- + 2I^- + 3H^+ \quad \text{Eq.2}$$

However, at high pH, the following reaction dominates.

$$I_2 + OH^- \rightarrow HOI + I^- \quad \text{Eq.3}$$

Most of the concern with respect to iodine in a nuclear system, is the potential loss of coolant accident that leads to the release of radio-iodine. In the disposal environment, where iodine could be present as a low level constituent, it could also impact the radiolysis chemistry for SNF disposal. In the case of iodine, thermodynamic understanding of iodine chemistry needs to consider the critical role of radiolysis, where the very fast reaction with OH•, results in volatilization of iodine. Indeed, under accident scenarios, iodine volatility is driven by this reaction [Wren et al., 2000].

2. RADIOLYSIS MODEL WITH IODINE REACTIONS

Previous work that reported the results of a radiolysis model sensitivity study [Wittman and Buck, 2012; Buck et al., 2013] showed that of the approximately 100 reactions [Pastina and LaVerne, 2001; Roth et al., 2012] describing water radiolysis, only about 37 are required to accurately predict H_2O_2 to one part in 10^5. The intended application of that radiolysis model (RM) was to calculate H_2O_2 production for an electrochemical based mixed potential model (MPM) [Jerden et al. 2012; 2013; 2015] developed to calculate the oxidation/dissolution rate of used nuclear fuel [Shoesmith et al., 2003; King and Kolar, 1999; 2002; 2003] under disposal conditions where O_2 is expected to be at low concentrations and H_2 is generated from oxidation of steel containers.

As an initial approximation, that model (MPM) was developed under the assumption that H_2O_2 is generated at a rate determined only by its radiolytic *G*-value. Ideally, for a full RM-MPM integration, the MPM would use a reaction kinetics based model to predict H_2O_2 for various water chemistries. As a further step in that direction, this report presents the effect of small concentration of halides on H_2O_2 concentration, leading from earlier studies reported by Buck and Wittman (2016) and explains the possible mechanism of that effect. Furthermore, we describe efforts to validate aspects of the RM with in-situ liquid cell electron microscopy experiments.

2.1 Effect of Iodide on H_2O_2 in Radiation Zone

To better understand how integration of the PNNL Radiolysis Model (RM) in the environment of iodine containing species can be integrated with the ANL Mixed Potential Fuel Degradation Model we consider iodine reactions in the RM. Since our goal is to consistently account for the chemistry in both models we focus on importance of the iodide ion on the generation of H_2O_2 affecting the UO_2 degradation rate.

The main approach is as follows.

- Identify the significant reactions that govern the chemical and radiolytic decomposition of H_2O_2 in water with known dose rate and concentrations of iodine species (Buxton and Mulazzani, 2007).
- Determine if iodine chemistry is well understood enough to accurately represent its effects on generation of H_2O_2 in the RM.

Progress on Bullet one (above) is summarized here and Bullet two is left as an open question.

Figure 2-1 uses the iodine reactions of Appendix A (Buxton and Mulazzani, 2007) within our current kinetics model to show the dependence of H_2O_2 concentration on the environmental concentration of iodide ions and bromide ions. Previous work has shown that the total number of reactions to consider can be reduced down from 77 for pure water to 38 (Elliot and McCracken, 1990; Christensen and Sunder, 1996; Wittman and Buck, 2012) together with the

approximately 30 additional iodine containing reactions (Buxton and Mulazzani, 2007). The bromide calculations from the model presented in (Buck and Wittman, 2016) have also been investigated by Kelm and Bohnert (2004).

Figure 2-1 shows both the bromide and iodide concentration effects on the radiolytic H_2O_2 concentration at 160 rad/s. For both ions the reduction in the steady-state H_2O_2 concentration continues with increased concentrations with the exception of micro-molar concentrations of bromide where even a 1 μM concentration can have a large effect. For these comparisons pH is fixed at 7.0 and anaerobic (1 μM O_2) conditions and a hydrogen (H_2) over-pressure (1 atm) were assumed. The effect of those conditions with diffusion out of the alpha radiation zone is currently being explored.

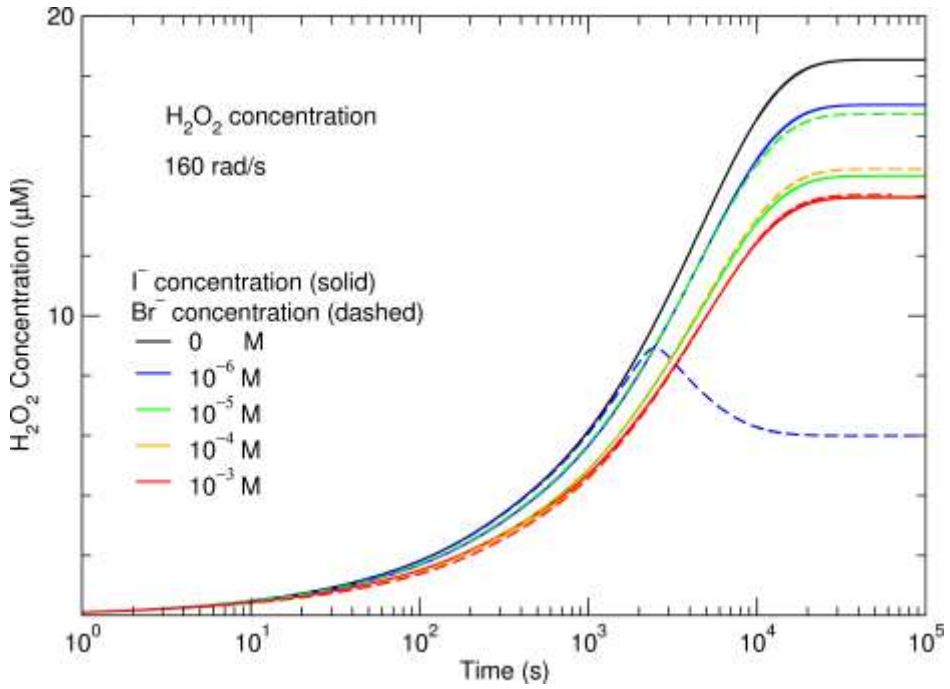

Figure 2-1. Effect of an initial micro-molar and greater concentration of Iodide (solid) and Bromide (dashed) ions on H_2O_2 generation at 160 rad/s alpha dose rate.

Figure 2-2 shows the H_2O_2 concentration with time at 25 rad/s to be proportionally lower by the dose rate ratios. The main difference is that the lower concentrations of bromide no longer significantly depletes O_2 at the fuel surface to allow H_2O_2 accelerated destruction.

At lower dose rate it would be expected that bromide and iodide ions will have similar effects on H_2O_2 concentration, whereas at higher dose rate even micro-molar concentration of bromide can a have a large effect.

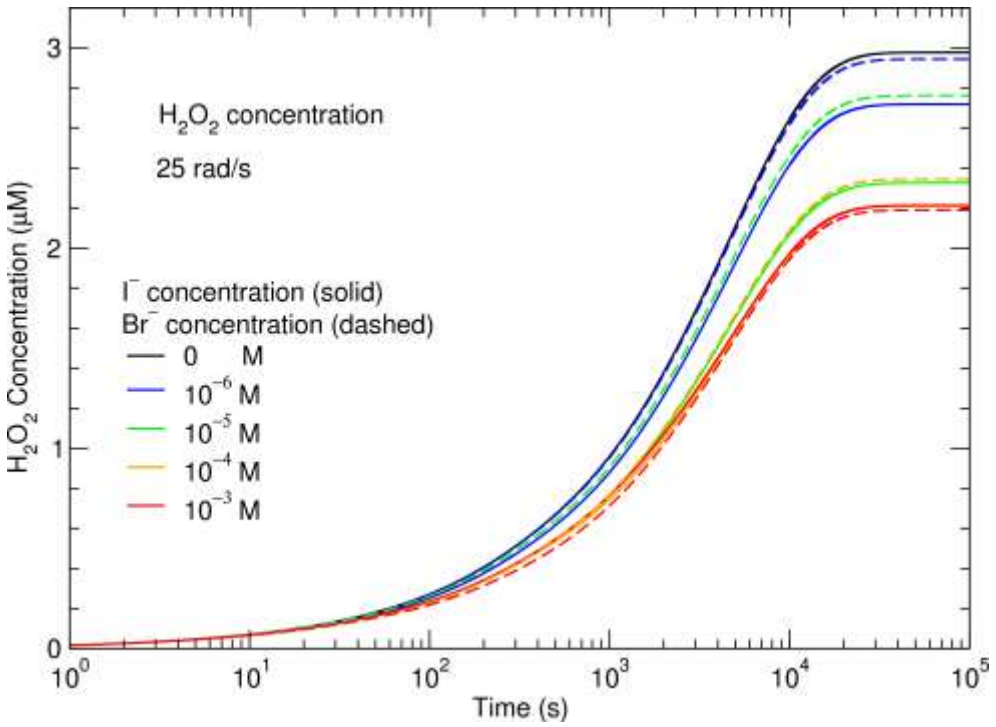

Figure 2-2. Effect of an initial micro-molar and greater concentration of Iodide (solid) and Bromide (dashed) ions on H_2O_2 generation at 25 rad/s alpha dose rate.

2.2 Experimental Validation of Radiolysis

Dissolution experiments were conducted using in-situ cells in the electron microscope to look for evidence of alteration in the presence of the electron beam. The use of *in-situ* liquid cells for investigating dissolution and precipitation phenomenon is well-established (Kimura et al. 2014). In this study, we used the QX-102 WetSEM cells from QuantomiX (Rehovot, Israel). Images were collected on an FEI (Thermo Fisher Scientific, Inc., Hilsboro, Oregon, USA) Quanta 250FEG Scanning Electron Microscope using backscattered imaging. To prevent rupturing the cells, a very low beam current was used. Powdered UO_2 (<45 µm sized sieved) was crushed between glass slides and suspended in DI water. The average size of the particles was <5 µm.

Figure 2-3 shows the investigation of the dissolution of UO_2 using an *in-situ* liquid cell. The UO_2 was exposed to a nitric acid solution at room temperature. Images were analyzed with Nikon Elements 4.0 software (Nikon Instruments, Inc. Melville, New York, USA) for the determination of particle size.

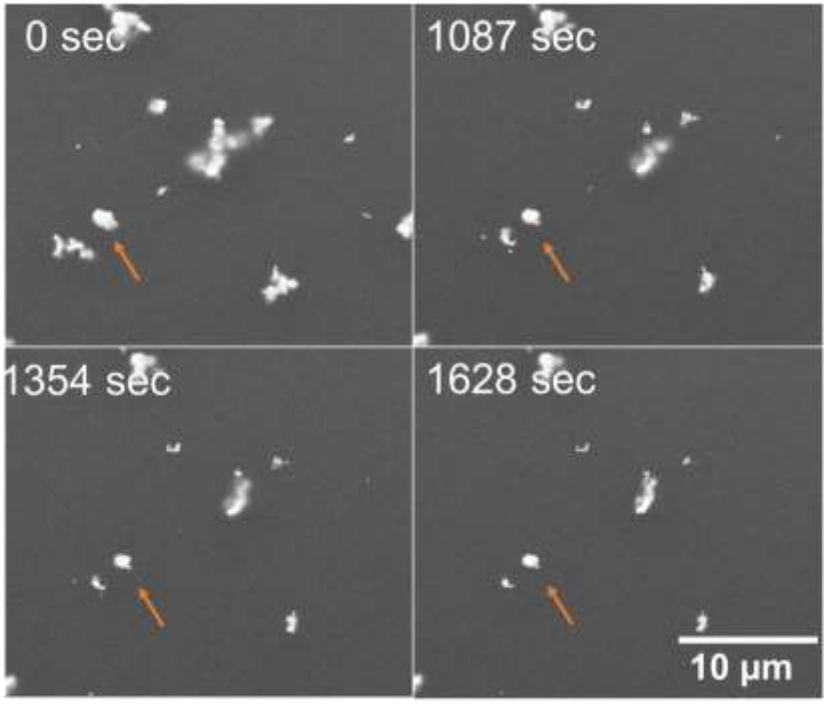

Figure 2-3 Tracking the dissolution of UO_2 in nitric acid showing how microscopy measurements can determine rates of reaction

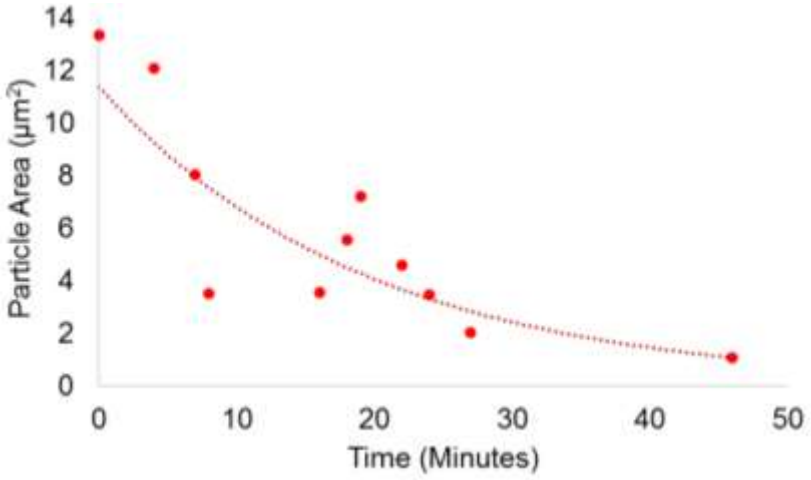

Figure 2-4 Plot showing change in particle surface area with time

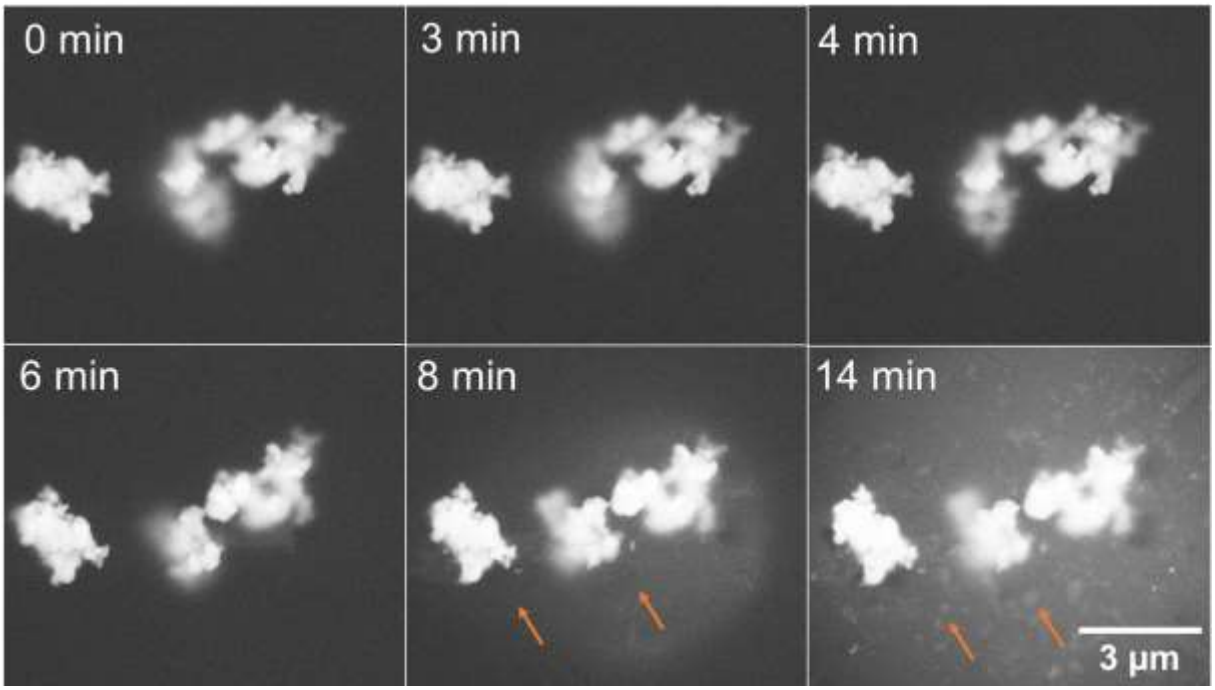

Figure 2-5 Electron microscopy images showing the formation of an alteration phase following the irradiation of a solution containing UO_2 particles.

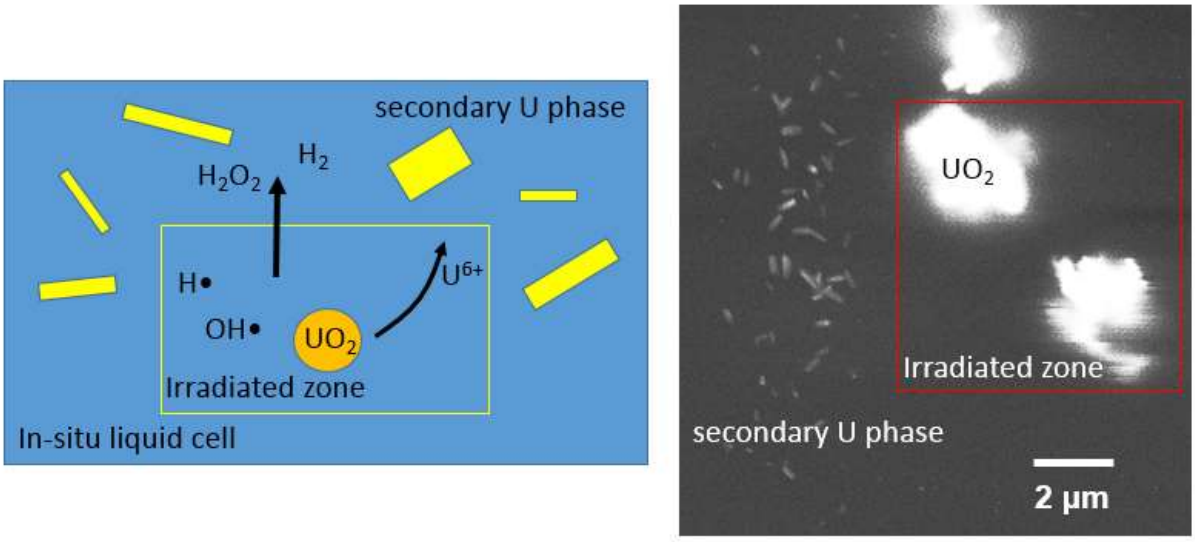

Figure 2-6 10 min Irradiation in a liquid cell with UO_2 in DIW.

During irradiation of DIW containing UO_2 particles, particles started to form outside the irradiated zone. These were elongated particles with an average length of 0.47±0.15 µm and width of 0.22±0.05 µm. The morphology of the particles is consistent with the expected secondary phase

under these conditions, studtite $[(UO_2)(O_2)(H_2O)_2](H_2O)_2$. The result from Figure 2-6 is in agreement with the RM code that indicated long lifetimes for H_2O_2 approximately 3 µm outside of the irradiated zone and where the radicals are rapidly annihilated. Furthermore, in these experiments, this result suggests that either the production of radical species locally is preventing the formation of the secondary phase or the electron beam is inducing destruction of the precursor phase preventing crystallization and growth.

2.3 Future work

While this work indicates that H_2O_2 production rates are relatively insensitive to iodide concentrations, it cannot guarantee that the mechanism operates under the repository conditions of spent nuclear fuel where additional chemical interactions are present. Future work would measure H_2O_2 generation in the presence of both bromide and iodide.

3. REFERENCES

Brown PN, and AC Hindmarsh. 1989. "Reduced storage matrix methods in stiff ODE systems." *Journal of Applied Mathematics and Computing*, 31(May 1989):40-91.

Buck, E.C, J.L. Jerden, W.L. Ebert, R.S. Wittman, (2013) "Coupling the Mixed Potential and Radiolysis Models for Used Fuel Degradation," FCRD-UFD-2013-000290, M3FT-PN0806058.

Buck, E.C., and Wittman, R.S. (2016), "Addition of Bromide to Radiolysis Model Formulation for Integration with the Mixed Potential Model", Pacific Northwest National Laboritory, PNNL-25539.

Buxton, G. V., Mulazzani, Q. G., (2007) On the hydrolysis of iodine in alkaline solution: A radiation chemical study, *Radiation Physics and Chemistry* 76: 932-940.

Christensen, H., Sunder, S. (1996) An evaluation of water layer thickness effective in oxidation of UO_2 fuel due to radiolysis of water, *Journal of Nuclear Materials* 238: 70-77.

Elliot, A.J.; McCracken, D.R. 1990, "Computer modelling of the radiolysis in an aqueous lithium salt blanket: Suppression of radiolysis by addition of hydrogen," Fusion Eng. Des., 13, 21.

Hindmarsh AC. 1983. "ODEPACK, A Systematized Collection of ODE Solvers." In *Scientific Computing*, IMACS Transactions on Scientific Computation, Volume 1 edited by RS Stepleman, M Carver, R Peskin, WF Ames and WF Vichnevetsky, North-Holland, Amsterdam, pp 55-64.

Jerden, J., Frey, K., Cruse, T., and Ebert, W. (2012). *Waste Form Degradation Model Status Report: Electrochemical Model for Used Fuel Matrix Degradation Rate*. FCRD-UFD-2012-000169.

Jerden, J., Frey, K., Cruse, T., and Ebert, W. (2013). *Waste Form Degradation Model Status Report: ANL Mixed Potential Model, Version 1. Archive*. FCRD-UFD-2013-000057.

Jerden, James L., Frey, Kurt, and Ebert, William (2015), *A multiphase interfacial model for the dissolution of spent nuclear fuel*, Journal of Nuclear Materials, 462: 135-146.

Kelm, M., E. Bohnert (2004), *A kinetic model for the radiolysis of chloride brine, its sensitivity against model parameters and a comparison with experiments*, Institut für Nukleare Entsorgung, Forschungszentrum Karlsruhe GmbH, Karlsruhe.

King, F. and Kolar, M. (1999) *Mathematical Implementation of the Mixed-Potential Model of Fuel Dissolution Model Version MPM-V1.0*, Ontario Hydro, Nuclear Waste Management Division Report No. 06819-REP-01200-10005 R00.

King, F. and Kolar, M. (2002) *Validation of the Mixed-Potential Model for Used Fuel Dissolution Against Experimental Data*, Ontario Hydro, Nuclear Waste Management Division Report No. 06819-REP-01200-10077-R00.
King, F. and Kolar, M. (2003) *The Mixed-Potential Model for UO2 Dissolution MPM Versions V1.3 and V1.4*, Ontario Hydro, Nuclear Waste Management Division Report No. 06819-REP-01200-10104 R00.

Kimura, Y., Niionmi, H., Tsukamoto, K., Garcia-Ruiz, J., (2014) In situ live observations of nucleation and dissolution of sodium chlorate nanoparticles by transmission electron microscopy, Journal of the American Chemical Society, 136, 1762-1765.

Pastina, B. and LaVerne, J. A. (2001) Effect of Molecular Hydrogen on Hydrogen Peroxide in Water Radiolysis, *Journal of Physical Chemistry* A105: 9316-9322.

Roth, O., Dahlgren, B., LaVerne, J. A., (2012) Radiolysis of water on ZrO2 nanoparticles, Journal of Physical Chemistry C, 116, 17619-17624.

Sassani et al., 2012 *Integration of EBS Models with Generic Disposal System Models*, U.S. Department of Energy, Used Fuel Disposition Campaign milestone report: M2FT-12SN0806062, September, 7 2012

Shoesmith, D.W., Kolar, M., and King, F. (2003). A Mixed-Potential Model to Predict Fuel (Uranium Dioxide) Corrosion Within a Failed Nuclear Waste Container, *Corrosion, 59*, 802-816.

Wittman RS and EC Buck. 2012. "Sensitivity of UO_2 Stability in a Reducing Environment on Radiolysis Model Parameters." In *Actinides and Nuclear Energy Material, MRS Spring 2012 Proceedings*, vol. 1444, 3-8, ed. D Andersson, et al. Cambridge University Press, Cambridge, United Kingdom. DOI:10.1557/opl.2012.1449.

Wren, J. C., Ball, J. M., Glowa, G. A., (2000) The chemistry of iodine containment, *Nuclear Technology*, 129, 297-325.

APPENDIX A:
Reaction Listing for Full RM

From: (Buxton and Mulazzani, 2007) & (Pastina and LaVerne, 2001)

```
Equilibrium constants:
H2O  <--> H+  +  OH- : RKeq(2) = 10^(-13.999)
H2O2 <--> H+  +  HO2-: RKeq(3) = 10^(-11.65)
OH   <--> H+  +  O-  : RKeq(4) = 10^(-11.9)
HO2  <--> H+  +  O2- : RKeq(5) = 10^(- 4.57)
H    <--> H+  +  E-  : RKeq(6) = 10^(- 9.77)
```

	Reactions	Rate constans (M^{-n}/s)
1	H+ + OH- = H2O	1.4d11
2	H2O = H+ + OH-	rk(2) = rk(1)*RKeq(2)
3	H2O2 = H+ + HO2-	rk(3) = rk(4)*RKeq(3)
4	H+ + HO2- = H2O2	5.0d10
5	H2O2 + OH- = HO2- + H2O	1.3d10
6	HO2- + H2O = H2O2 + OH-	rk(6) = rk(5)*RKeq(2)/RKeq(3)
7	E- + H2O = H + OH-	1.9d1
8	H + OH- = E- + H2O	2.2d7
9	H = E- + H+	rk(9) = rk(10)*RKeq(6)
10	E- + H+ = H	2.3d10
11	OH + OH- = O- + H2O	1.3d10
12	O- + H2O = OH + OH-	rk(12) = rk(11)*RKeq(2)/RKeq(4)
13	OH = O- + H+	rk(13) = rk(14)*RKeq(4)
14	O- + H+ = OH	1.0d11
15	HO2 = O2- + H+	rk(15) = rk(16)*RKeq(5)
16	O2- + H+ = HO2	5.0d10
17	HO2 + OH- = O2- + H2O	5.0d10
18	O2- + H2O = HO2 + OH-	rk(18) = rk(17)*RKeq(2)/RKeq(5)
19	E- + H2O2 = OH + OH-	1.1d10
20	E- + O2- + H2O = HO2- + OH-	1.3d10
21	E- + HO2 = HO2-	2.0d10
22	E- + O2 = O2-	1.9d10
23	H + H2O = H2 + OH	1.1d1
24	H + H = H2	7.8d9
25	H + OH = H2O	7.0d9
26	H + H2O2 = OH + H2O	9.0d7
27	H + O2 = HO2	2.1d10
28	H + HO2 = H2O2	1.8d10
29	H + O2- = HO2-	1.8d10
30	OH + OH = H2O2	3.6d9
31	OH + HO2 = H2O + O2	6.0d9
32	OH + O2- = OH- + O2	8.2d9
33	OH + H2 = H + H2O	4.3d7
34	OH + H2O2 = HO2 + H2O	2.7d7
35	HO2 + O2- = HO2- + O2	8.0d7
36	H2O2 = OH + OH	2.25d-7
37	OH + HO2- = HO2 + OH-	7.5D9
38	HO2 + HO2 = H2O2 + O2	7.0d5
38	HO2 + HO2 = H2O2 + O2	7.0d5
39	HOI + OH- = IO- H2O	1.3d10
40	IO- H2O = HOI + OH-	1.0d5
41	I + I- = I2-	9.1d9
42	I2- = I + I-	6.7d4
43	I2 + I- = I3-	6.2d9
44	I3- = I2 + I-	8.7d6
45	I2 + OH- = I2OH-	1.d10

46	I2OH- = I2 + OH-	4.4d6
47	I2OH- = HOI + I-	5.4d6
48	HOI + I- = I2OH-	3.d8
49	I2 + HO2- = HOOI + I-	4d8
50	HOOI + I- = I2 + HO2-	5d5
51	HOI + HO2- = HOOI + OH-	2.1d9
52	HOOI + OH- = I- + O2 + H2O	2d9
53	OH + I- = HOI-	1.6d10
54	I- + O- + H2O = HOI- + OH-	2.0d9
55	HOI- = I + OH-	3.5d7
56	I + OH- = HOI-	1.6d8
57	I + I = I2	1.1d10
58	I + I2- = I3-	6.5d9
59	I2- + I2- = I3- + I-	2.5d9
60	O2- + I2 = O2 + I2-	6.0d9
61	O2- + I3- = O2 + I2- + I-	2.5d8
62	H + I2 = I2- + H+	3.5d10
63	H + I3- = I- + I2- + H+	3.5d10
64	E- + I2 = I2-	5.1d10
65	E- + I3- = I- + I2-	3.5d10
66	OH + I2 = HOI + I	1.1d10
67	OH + I3- = I2- + HOI	1d10
68	E- + HOI = OH- + I	2d10
69	E- + IO- = I- + O-	1.6d10
70	H + HOI = I + H2O	1d9
71	OH + HOI = HOIOH	7d9
72	HOIOH = IO + H2O	1.3d6
73	HOI + HOI + OH- = IO2- + I- + H+ + H2O	5.6
74	IO2- + HOI = IO3- + I- + H+	1d3
75	IO + IO = I2O2	1.5d9
76	I2O2 + H2O = HOI + IO2- + H+	1d4
77	H + I2- = H+ + I- + I-	1.8d7

APPENDIX B:
FORTRAN Listing for Empirical RM

Emp-RM.f

```
      implicit real*8 (a-h,o-z)

      ddot  = 160.d0          ! rad/s


      Brext = 1.d-6

      do i=0,200
      do j=0,200

      H2ext = 7.8d-4*dfloat(j)/100.d0      ! mole/L
      O2ext = dfloat(i)/2.d7 +  1.d-11     ! mole/L
      G2 = Gcond(ddot,O2ext,H2ext,Brext)

      write(*,*) H2ext,O2ext,G2

      enddo
      write(*,"(1x)")
      enddo


      STOP
      end

      FUNCTION Gcond(ddot,O2ext,H2ext,Brext)
      implicit real*8 (a-h,o-z)


      rk27   = 2.1d10         ! L/mole-s
      rk23   = 1.1d1/56.d0    ! L/mole-s   divided by 56
      rk26   = 9.0d7          ! L/mole-s
      rk36   = 0.0d0          ! L/mole-s
      rk33   = 4.3d7
      rk94   = 1.1d10 * 10.
      BrFact = rk33*H2ext/(rk33*H2ext + rk94*Brext)
      if(Brext.eq.0.) BrFact = 1.d0
      GH    = 0.100d0*(1.d0-dexp(-(H2ext*BrFact/7.8d-4)/.1d0))         ! molecules/eV
      GOH   = 0.350d0*(1.d0-dexp(-(H2ext*BrFact/7.8d-4)/.3d0))         ! molecules/eV
      CH2O  = 1.d3/18.d0      ! mole/L
      DO2   = 2.500d-05       ! cm^2/s
      DH2O2 = 1.900d-05       ! cm^2/s
      dx    = 3.5d-3          ! cm
      dN    = 0.475d0/dx
      GOH   =   GOH  * BrFact

         O2 =  O2ext + 2.d-6*Brext/(Brext+0.5d-6)
         H2 =  H2ext
         H2O = CH2O
         dk27   =  rk27
         dk23   =  rk23
         dk26   =  rk26
         dk36   =  rk36
      dkO2   =   DO2/(dN*dx**2)        !  1/s
      dkH2O2 =   DH2O2/(dN*dx**2)      !  1/s
      dot=   ddot*(1.d0/(1.602d-19*1.d4*6.022d23))


      A0 =      -dk23*dk27*H2O*dkH2O2**2
```

```
      A1 = -dkH2O2*(dk26*dk27*dkO2*O2+dk23*dk26*dkO2*H2O
     1   - 2.d0*(dk23*dk27*H2O)*(dkH2O2+dk36) )
     2   + dot*(gH+gOH)*dk26*dk27*dkH2O2

      A2 =  (dkH2O2+dk36)*(dk26*dk27*dkO2*O2+dk23*dk26*dkO2*H2O
     1   - (dk23*dk27*H2O)*(dkH2O2+dk36) )
     2   + dot*(gH+gOH)*dk26*(dk26*dkO2-dk27*dkH2O2-dk27*dk36)

      Gcond =  (-A1 + dsqrt(A1**2 - 4.d0*A2*A0))/(2.d0*A2)
c      Gcond = dkH2O2/(dkH2O2+dk36+dk26*dot*(gOH+gH)/
c     1     (dk23*H2O+dk27*O2))

      RETURN
      end

      SUBROUTINE NLconc(C1p,C1m,C0,dlam0,A,dN,dk)
      implicit real*8 (a-h,o-z)

      B = -(1.d0 - 1.d0/(A*C0) - dN*dlam0/(dk*A*C0))
      C = -1.d0/(A*C0)

      C1p = ( -B + dsqrt(B**2 - 4.d0*C) )/2.d0
      C1m = ( -B - dsqrt(B**2 - 4.d0*C) )/2.d0


      RETURN
      end
```